25th ABCM International Congress of Mechanical Engineering
October 20-25, 2019, Uberlândia, MG, Brazil

# COB-2019-0196
# NUMERICAL EVALUATION OF STRESS CONCENTRATION FACTOR FOR DIFFERENT DESIGNS OF SHAFT SHOULDER APPLIED TO RADIAL BEARINGS HOUSINGS

**Guilherme Cesar do Amaral Dias**
**João Luiz do Vale**
**Jéderson da Silva**

Federal Technological University of Paraná. Londrina, 86036 370, PR. Brasil.
e-mails: guilhermedias@alunos.utfpr.edu.br, joaovale@utfpr.edu.br, jedersonsilva@utfpr.edu.br.

***Abstract.*** *This article proposes a methodology for a numerical evaluation of stress concentration factors in shafts with respect to the application of radial bearings under three conditions of pure load: traction, bending and torsion. In this case, the simple fillet bearing shoulder is compared to two designs established in technical standards. A numerical model was defined and carried out in Ansys® software. Through the comparison with data provided in literature, a validation of the numerical model for the simple fillet shoulder was performed. A planning of the numerical experiment is described in order to meet a range of geometric parameters linked to data provided in radial bearing catalogs. A comparison between the simple fillet concentration factors versus standardized designs is provided by defining a percentual measure. The results of numerical validation experiments demonstrated the effectiveness of the proposed methodology. Additionally, it is shown that the use of the simple fillet presents, in some cases, lower stress concentration factors than those generated by the designs proposed by the standard.*

***Keywords:*** *Stress concentration, Shaft shoulder, Radial bearings, Finite element analyses.*

## 1. INTRODUCTION

For a machine designer, a fairly common task is to dimension a shaft. To that end, various considerations must be evaluated, among them the determination of stress levels imposed by the loads, and especially the influence of stress intensifiers play a fundamental role (Allison, 1961; Norton, 2010). Indeed, in practice, machine elements are often attached to shaft with steps — which guarantee positioning accuracy but impose stress intensifiers. Recent literature analysis related to the evaluation of stress concentration factors in shafts are presented by Ajovalasit et al. (2014) and Abhyankar and Deshmukh (2017). In this context, it must be highlighted the demands for bearings, whose positions on a shaft, are obtained with shaft shoulder. Thereby, considering a simple fillet design and the bearing assembly demands, the largest fillet radius allowable in a shaft shoulder must be smaller than the smallest radius of edge of the inner ring of the bearing (SKF, 1989). Even though this type of fillet design presents, as advantages, a low-cost and simplicity of manufacture, its geometry constraint leads to higher stress concentrations factors (Pilkey and Pilkey, 2008). Fortunately, there are some fillet design options that allow the use of larger radius. Moreover, one can find standardized proposals such as DIN 509 (1998) which also provides geometrical data. Nonetheless, there is a lack in the literature with respect to their stress concentration factors. An alternative for the evaluation of stress concentration factors is the use of numerical methods, such as the Finite Element Method, the Finite Difference Method and the Boundary Element Method (Ajovalasit et al., 2014). In particular, Deshpande et al. (2016) discuss the influence of different types of finite elements on the precision of the numerical evaluation of stress concentration factors applied to a central bore plate subjected to axial loading.

This work has the objective of evaluating two different standard designs for radial bearings regarding the intensity of stress concentration factors and compare them with the simple fillet. A procedure for planning a numerical experiment, carried out in Ansys® software, was proposed in order to cover geometrical parameters of the problem in question. Furthermore, a validation was done by comparing results found in the literature for the simple fillet.

## 2. METHODOLOGY

### 2.1 Main definitions and geometrical aspects of the designs for the proposed shaft shoulders

Stress concentration factor was evaluated for three types of pure loading: traction, bending and torsion whose formulations for determination of nominal stress are presented, respectively, in Equation (1):

$$\sigma_{nom} = 4F/\pi d^2, \quad \sigma_{nom} = 32M/\pi d^3, \quad \tau_{nom} = 16T/\pi d^3, \tag{1}$$

where $\sigma_{nom}$ represent nominal stress for traction and bending [MPa], $\tau_{nom}$ the nominal stress for torsion [MPa], $d$ the inner diameter of the shaft [mm], $F$ the traction force [N], $M$ the bending moment [Nm] and $T$ the torque [Nm].

These are the most common loads imposed on shafts according to the basic literature (Abhyankar and Deshmukh, 2017). Attention should be paid to the classical formulae presented here for the specific case of circular section shaft. Obviously, these pure loads can be combined by applying the principle of overlapping effects since the material is kept under its elastic regime (Hibbeler, 2015). The geometric stress concentration factors, also in the classical formulation (Norton, 2010; Hibbeler, 2015), were considered as the ratio between the maximum local stress and the nominal stress as shown in Equation (2):

$$K_{tn} = \sigma_x/\sigma_{x_{nom}}, \quad K_{ts} = \tau_{xy}/\tau_{xy_{nom}}, \tag{2}$$

where $K_{tn}$ and $K_{ts}$ represent, respectively, the geometric stress concentration factor for normal and shear stress.

Hereby, it is worth mentioning that different definitions for the evaluation of concentration factors are found in the literature (e.g. Young and Budynas, 2002; Yang et al., 2008), which can be defined on the basis of deformation, strain or both.

Geometric stress concentration factors were investigated for two selected designs of proposed shaft shoulder in DIN 509 (1998) (Design A and Design C), which are shown in Figure 1(a-b); where $D$ and $r$ represent, respectively, diameter and radius of the shoulder. By the authors' interpretation these two forms have representative geometric aspects of other designs proposed in this standard. In addition, comparisons were made with the more common design used for shaft shoulder, named here as simple fillet, which is presented in Figure 1(c).

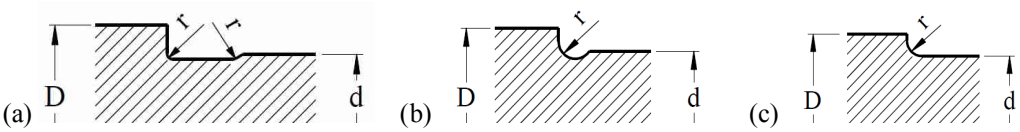


Figure 1. Shaft shoulder designs evaluated: (a) Design A – Din 509, (b) Design C – Din 509 and (c) Simple fillet.

For a more coherent study of shaft shoulders specifically for the application of bearings, some geometrical data was collected — with respect to the parameters, *r/d* and *D/d* — from manufacturers catalogs (SKF, 2003). This information was relevant for planning a numerical experiment, which is presented in Section 2.2. In this fashion, some restrictions were imposed on the data collection. First, only the main radial bearings were taken into account: deep-groove ball bearings, cylindrical roller bearings, angular contact ball bearings, tapered roller bearing, self-aligning ball bearings, and self-aligning roller bearings. Second, it was arbitrated a range for the inner diameter (*d*) from the smallest size (10 mm) up to 100 mm — the result is summarized in the Figure 2 — and considering that, smaller values of *r/d* and *D/d* impose a more critical condition for stress concentration factors. Figure 2 is helpful to evidence that more attention must be paid to deep-groove ball bearings and angular contact ball bearings since they present the most critical conditions.

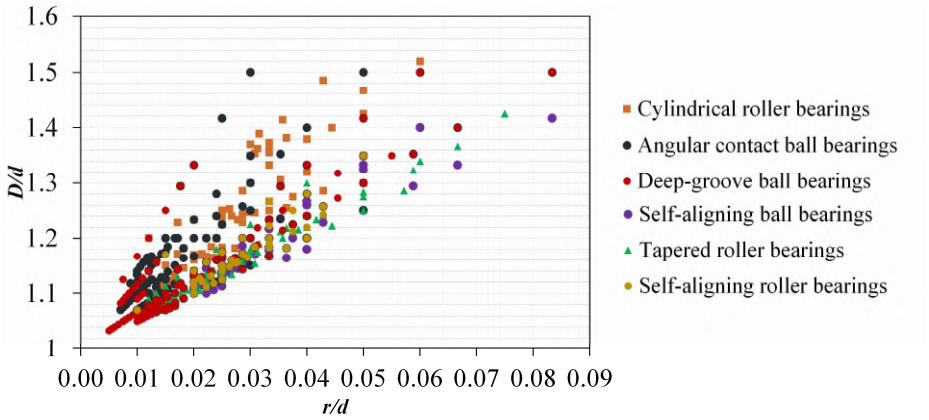


Figure 2. Geometrical parameters collected from manufacturers' catalogs for main radial bearings.

### 2.2 Planning of the numerical experiment, numerical model and validation

The numerical experiment for the simple fillet, presented in Figure 3, was planned in a factorial manner in order to sweep the ranges identified for *r/d* and *D/d* presented in Figure 2. For the selected designs of the standard, by their turn, the numerical experiment was a combination of the seven levels of *D/d*, pointed out in Figure 3, with the options of radii proposed by the standard. The radii options are summarized in Table 1. With this planning, 126 simulations were performed for the simple fillet and 138 for both designs of the standard.

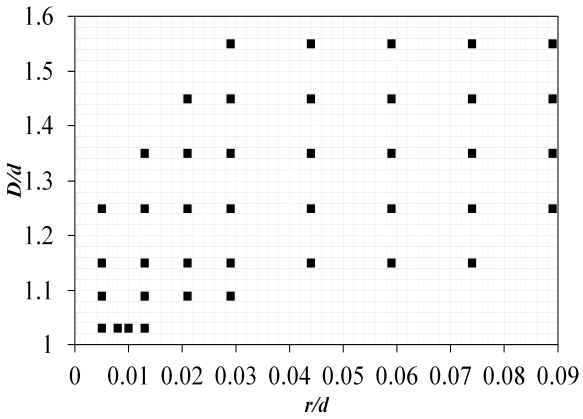


Figure 3. Planning of numerical experiment for the simple fillet.

Table 1. Radii options proposed by DIN 509 standard.

| Design A [mm] | Design C [mm] |
|---|---|
| 0.2 | 1.0 |
| 0.4 | 1.6 |
| 0.6 | 2.5 |
| 1.0 | |

The simulation results were presented in graphs of *D/d* versus *r/d*. In addition, a potential-type curve, according to Equation (3), was fit to the results and the constants A and b were provided as well as their determination coefficients ($R^2$).

$$K_{tn} = K_{ts} = A\left(\frac{r}{d}\right)^b \tag{3}$$

The finite element analysis was conducted in evaluations under elasticity laws and performed using Ansys®. The main simulation parameters are summarized in Table 2. The shaft was modeled with mechanical properties typically associated with steel alloys. Besides that, both the dimensions of the model (such as shaft length and inner diameter) and the nominal stress value (for all types of loads) were kept constant and were arbitrarily defined. The models were meshed with tetrahedral elements of second order. Using finite elements of higher order, for this study, is a viable approach due to the minimization of domain discretization error (Zienkiewicz and Taylor, 2000). Initially, a general mesh was created with elements size of approximately 5 mm, and then an h-refinement (with element size of 0.5 mm) was imposed only to the surface of the shoulder radius. This procedure aimed to facilitate the stress convergence obtained by a mesh convergence tool, available in the software, which was set to Normal Stress. An advantage of the h-refinement is to achieve the convergence with fewer iterations and to avoid that the maximum tension stress could be found in the fixed support, for instance, instead of the shaft shoulder. Still in this convergence context, one should keep it in mind that the order of the finite element also has influence — being that the higher the order of the element, the faster is the convergence (Zienkiewicz and Taylor, 2000).

Table 2. Overall simulation parameters used for FEA.

| **Parameter** | **Value** |
|---|---|
| Young's Modulus [MPa] | 200000 |
| Poisson's Ratio [-] | 0.3 |
| Inner diameter [mm] | 50 |
| Length of the inner diameter [mm] | 50 |
| Length of the shaft [mm] | 100 |
| r/d and D/d | According to presented in section 2.2 |
| Element finite type | Tetrahedron with 10 nodes (Tet10 Ansys®) |
| Nominal stress [MPa] | 100 |
| Boundary conditions applied to the shaft | Fixed at the bigger end |
| Allowable convergence change in von Mises Stress [%] | 0.5 |

A validation procedure of this numerical model was performed for the simple fillet due to the possibility of comparison with literature. Although several books provide equations for determining the stress concentration factor for simple fillet (Young and Budynas, 2002; Pilkey and Pilkey, 2008; Norton, 2010). In this work, the reference's data used for validation is described by Pilkey and Pilkey (2008). Therefore, a percentage error was presented for the three types of pure loads, for six conditions of *r/d* arbitrarily distributed to the range of 0.02 to 0.095 and for *D/d* = 1.2.

## 3. RESULTS AND DISCUSSION

### 3.1 Numerical model validation

Based on the methodology and simulation parameters described in section 2, Figure 4 presents the results regarding the numerical model validation. This model considers a shaft with a simple fillet shoulder under three conditions of pure loads: traction force, bending moment and torsion moment.

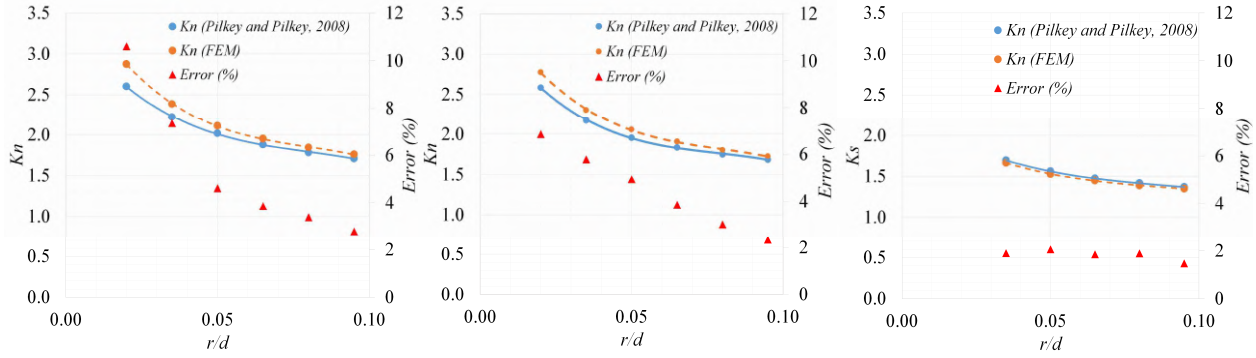


Figure 4. Validation of the proposed numerical model, applied to simple fillet, for pure loadings of: (a) traction force, (b) bending moment and (c) torsion moment.

In it is observed that the numerical model has a behavior similar to those presented by Pilkey and Pilkey (2008), indicating an increase in the intensity of the stress concentration factor with the reduction of the fillet radius. It is noticed that for identical nominal tension and geometry, traction and bending loads generate larger values for the stress concentration factor when compared to the torsional load. In this case, besides the comparison between the theoretical and numerical curves, values of percentage errors between both methodologies are shown. Above all, it is worth mentioning that there is a tendency of increased error for smaller radius, being that, the traction load presents the maximum error of 10.61%.

Another aspect related to the validation of the numerical model is the convergence of the maximum value of stress. In this context, considering a bending moment, presents a normal stress distribution for the geometry under analysis and a history of convergence for the largest and smallest radii of the experiment described in Figure 3. In this case, the location of the maximum stress occurred, as indicated in the literature, in the abrupt region of the cross-sectional area of the shaft (Figure 5. (a)). This fact indicates the correct application of the Dirichlet contour conditions at the left end of the shaft, which, if mistakenly applied, can generate stress concentrators. Regarding the numerical experiments performed, it is observed that the imposition of a fine initial finite element mesh in the fillet region results in a low maximum normal variation. Moreover, in Figure 5. (b) a larger number of iterations is required when using smaller radii. When referring to 1.0 mm radius, the variation in the maximum stress between iteration 2 and 3 is only 0.78%. In this case, in order to reach a percentage variation value below 0.5%, a significant increase in the number of elements of the mesh was required. On that account, for the numerical experiments conducted, in order to compare the different forms of construction of bearing rests, an acceptable value of 1% was adopted in the variation of maximum normal stress.

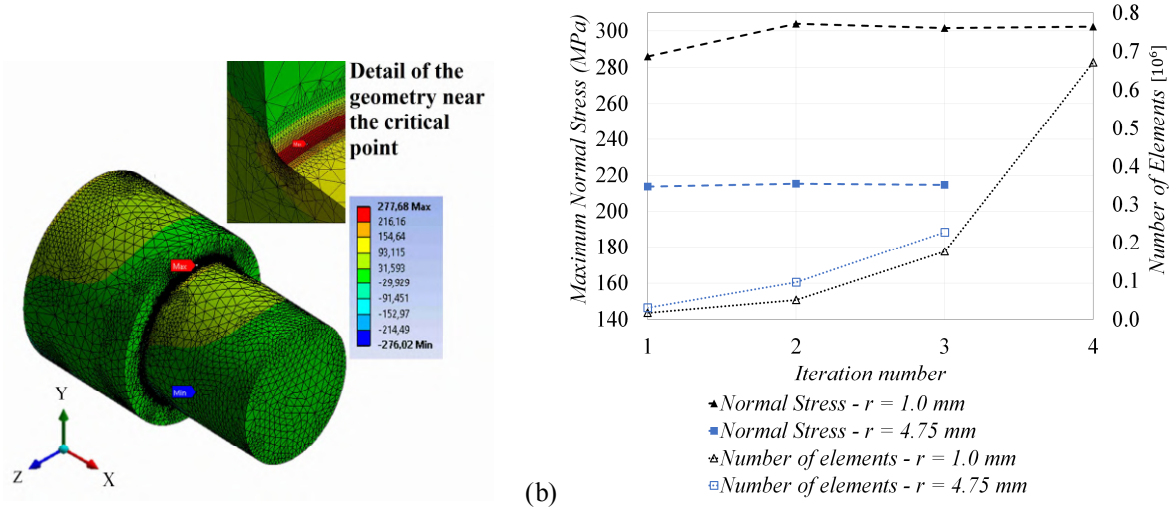


Figure 5. Shaft with simple fillet shoulder ($d$ = 50 mm and D = 60 mm) subjected to bending load: (a) Normal stress distribution and critical point location for $r$ = 1.0 mm and (b) Convergence history for $r$ = 1.0 mm and $r$ = 4.75 mm.

### 3.2 Stress concentration factors

Figures 6, 7 and 8 present the stress concentrator factors, respectively, for the simple fillet and designs A and C of DIN 509, for pure traction force, bending moment and torsion moment. In general, it can be observed that tension concentrators for traction force and bending moment are more critical for all evaluated designs. Attention is drawn to the fact that due to the radii proposal indicated by DIN 509 (Table 1), the domains of the graphs in relation to *r/d* are more restricted to the standard designs in application for the shoulders of the main types of radial bearings.

Along with the graphs, data from the trend curves according to Equation (3) are presented. The high values of the determination coefficients ($R^2$) show a high representativity setting for a potential-curve type. Thus, these results provide the possibility of evaluations of the concentrators without the need of simulations.

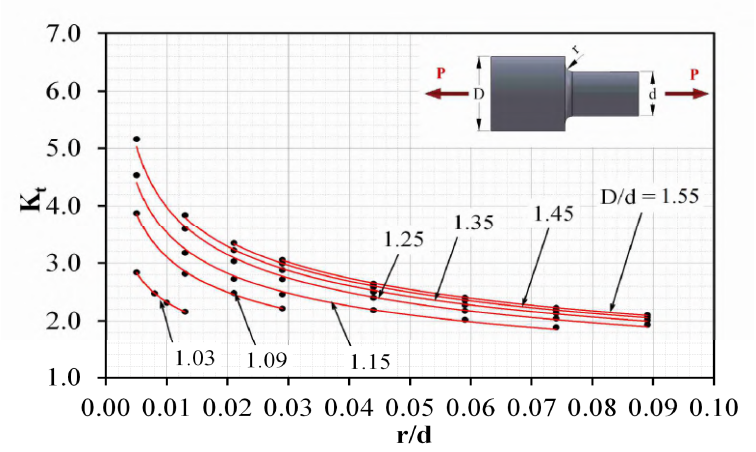


| D/d | A | b | $R^2$ |
|---|---|---|---|
| 1.55 | 0.83621 | -0.36153 | 0.999 |
| 1.45 | 0.82670 | -0.35760 | 0.999 |
| 1.35 | 0.80440 | -0.35532 | 0.998 |
| 1.25 | 0.75843 | -0.35765 | 0.996 |
| 1.15 | 0.72656 | -0.34038 | 0.993 |
| 1.09 | 0.64380 | -0.33526 | 0.999 |
| 1.03 | 0.59114 | -0.28729 | 0.999 |

(a) Traction concentration factors

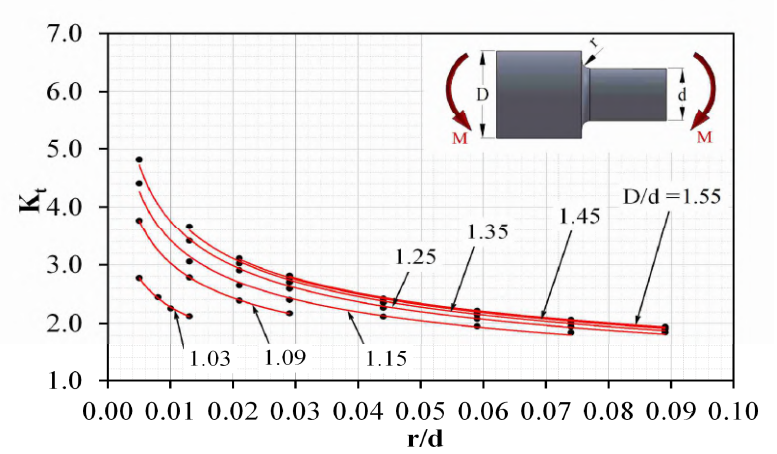


| D/d | A | b | $R^2$ |
|---|---|---|---|
| 1.55 | 0.87772 | -0.32794 | 0.999 |
| 1.45 | 0.86088 | -0.33137 | 0.999 |
| 1.35 | 0.83098 | -0.33726 | 0.997 |
| 1.25 | 0.81482 | -0.33179 | 0.998 |
| 1.15 | 0.78471 | -0.31988 | 0.994 |
| 1.09 | 0.71605 | -0.31316 | 0.999 |
| 1.03 | 0.61514 | -0.28471 | 0.996 |

(b) Bending concentration factors

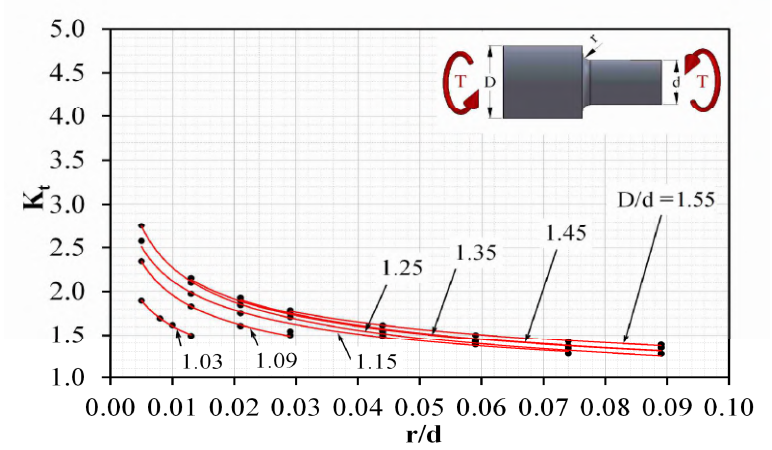


| D/d | A | b | $R^2$ |
|---|---|---|---|
| 1.55 | 0.78664 | -0.23045 | 0.997 |
| 1.45 | 0.70051 | -0.25954 | 0.979 |
| 1.35 | 0.70481 | -0.25555 | 0.990 |
| 1.25 | 0.64770 | -0.27255 | 0.996 |
| 1.15 | 0.68908 | -0.24409 | 0.985 |
| 1.09 | 0.59991 | -0.25707 | 0.999 |
| 1.03 | 0.51965 | -0.24481 | 0.996 |

(c) Torsion concentration factors

Figure 6 - Stress concentration factors for simple fillet.

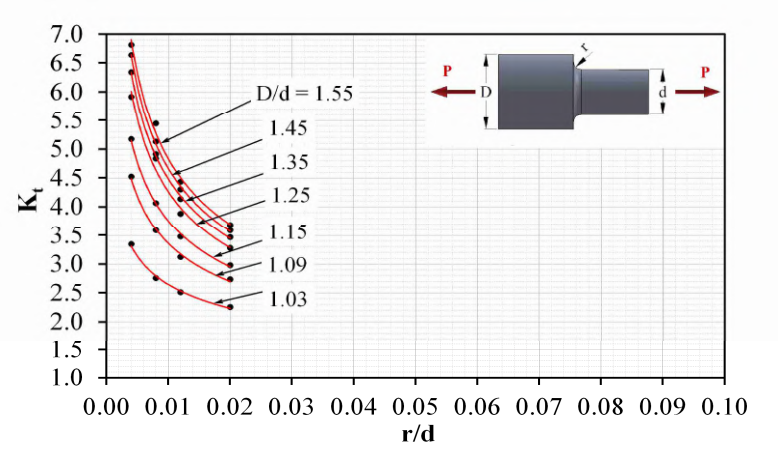


| D/d | A | b | $R^2$ |
|---|---|---|---|
| 1.55 | 0.80561 | -0.38906 | 0.993 |
| 1.45 | 0.79046 | -0.38555 | 0.999 |
| 1.35 | 0.78340 | -0.37875 | 0.999 |
| 1.25 | 0.75486 | -0.37583 | 0.986 |
| 1.15 | 0.76327 | -0.34588 | 0.998 |
| 1.09 | 0.78616 | -0.31540 | 0.997 |
| 1.03 | 0.85508 | -0.24523 | 0.995 |

(a) Traction design A

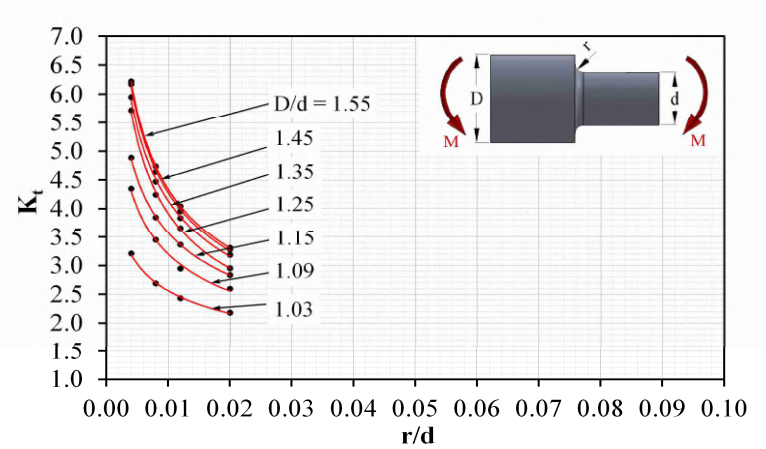


| D/d | A | b | $R^2$ |
|---|---|---|---|
| 1.55 | 0.71213 | -0.39259 | 0.999 |
| 1.45 | 0.69932 | -0.39342 | 0.999 |
| 1.35 | 0.69312 | -0.38807 | 0.999 |
| 1.25 | 0.59692 | -0.40848 | 0.999 |
| 1.15 | 0.75351 | -0.33825 | 0.999 |
| 1.09 | 0.71526 | -0.32555 | 0.993 |
| 1.03 | 0.84546 | -0.24076 | 0.998 |

(b) Bending design A

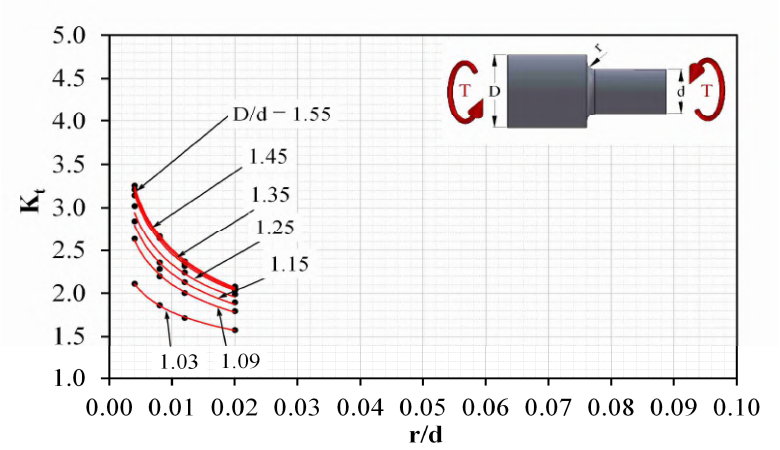


| D/d | A | b | $R^2$ |
|---|---|---|---|
| 1.55 | 0.69294 | -0.27944 | 0.999 |
| 1.45 | 0.69378 | -0.27703 | 0.999 |
| 1.35 | 0.69872 | -0.27300 | 0.998 |
| 1.25 | 0.72435 | -0.25405 | 0.965 |
| 1.15 | 0.70581 | -0.24950 | 0.984 |
| 1.09 | 0.70449 | -0.23744 | 0.997 |
| 1.03 | 0.76654 | -0.18342 | 0.999 |

(c) Torsion design A

Figure 7. Stress concentration factors for design A.

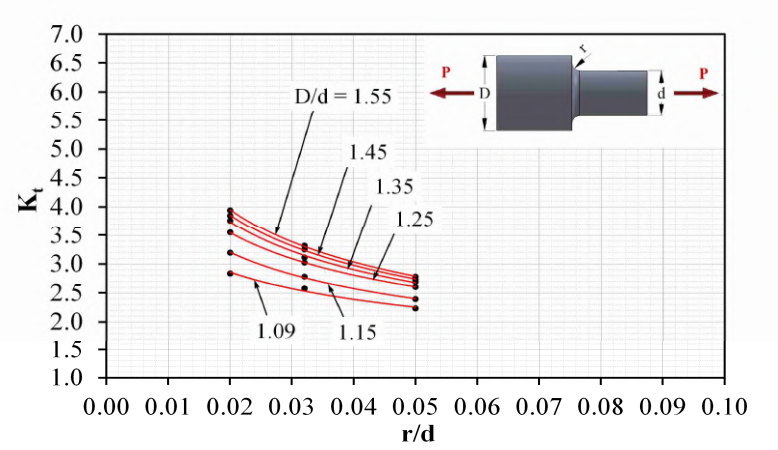


| D/d | A | b | $R^2$ |
|---|---|---|---|
| 1.55 | 0.89188 | -0.38038 | 0.999 |
| 1.45 | 0.89546 | -0.37315 | 0.999 |
| 1.35 | 0.89643 | -0.36495 | 0.996 |
| 1.25 | 0.95110 | -0.33621 | 0.999 |
| 1.15 | 0.93235 | -0.31553 | 0.998 |
| 1.09 | 1.03522 | -0.25966 | 0.983 |

(a) Traction design C

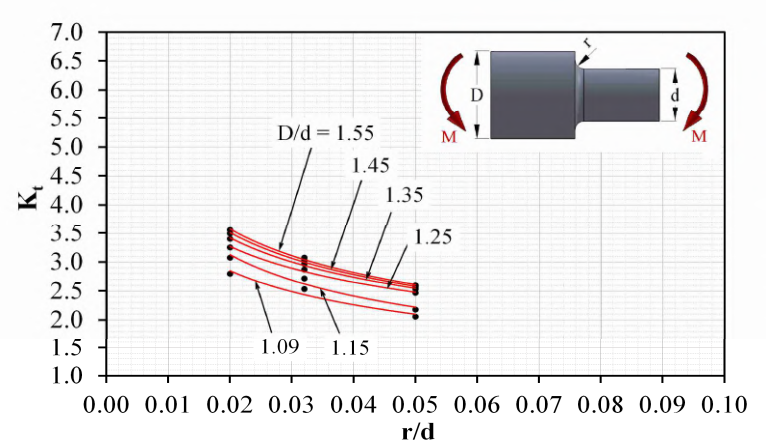


| D/d | A | b | $R^2$ |
|---|---|---|---|
| 1.55 | 0.93638 | -0.34215 | 0.996 |
| 1.45 | 0.94362 | -0.33574 | 0.998 |
| 1.35 | 0.97210 | -0.32134 | 0.996 |
| 1.25 | 1.00086 | -0.30247 | 0.995 |
| 1.15 | 0.72380 | -0.37391 | 0.971 |
| 1.09 | 0.77211 | -0.33366 | 0.953 |

(b) Bending design C

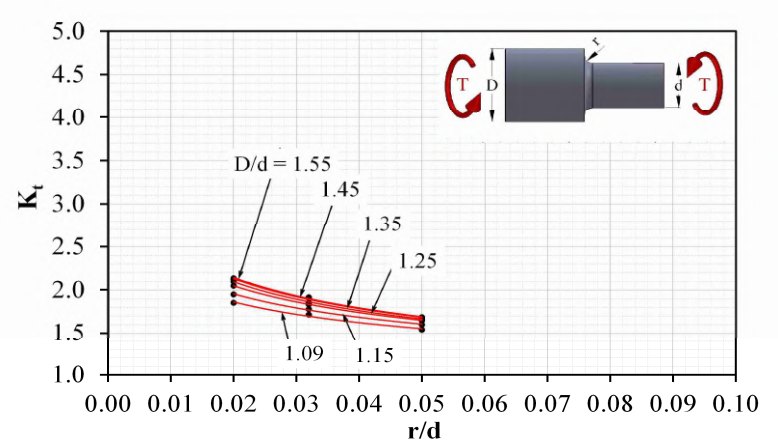


| D/d | A | b | $R^2$ |
|---|---|---|---|
| 1.55 | 0.77723 | -0.25952 | 0.997 |
| 1.45 | 0.78419 | -0.25537 | 0.994 |
| 1.35 | 0.78845 | -0.24961 | 0.999 |
| 1.25 | 0.81527 | -0.23534 | 0.999 |
| 1.15 | 0.84595 | -0.21401 | 0.996 |
| 1.09 | 0.85855 | -0.19781 | 0.988 |

(c) Torsion design C

Figure 8. Stress concentration factors for design C.

### 3.2.1 Comparison between designs

An important task in selecting a type of bearing shoulder design is to know what the gain or loss would be in relation to the stress concentration factor. In order to compare the stress concentration factors between the designs, a percentual relation was established as presented in Equation (4). Noteworthy that with this formula, positive values mean increase of the stress concentration in relation to the simple fillet design.

$$1 - \left(\frac{K_{t\,simple\,fillet}}{K_{t\,standard}}\right)[\%] \tag{4}$$

Before presenting the comparison data, it is still necessary to understand what are the possible options for the designs of the standard that can be an alternative to a certain simple fillet geometry. In fact, the data presented in Figure 2 referring to the simple fillet are associated to the larger radius allowed for the assembly of the bearings, which results in the smaller factor of concentration of stress taking into account the constraint imposed by the assembly. However, the designs of the standard shown in Figure 1(a-b) eliminate the maximum radius restriction for bearing assembly. With this, it is possible to apply all radii options indicated by the standard (Table 1).

Based on this context, comparisons are presented for extreme cases of *D/d* evaluated in this work (i.e. 1.09 and 1.55). Figure 9 and Figure 10 (a-c) show the absolute values of stress concentration factors for the three designs evaluated for each type of loading and *D/d*. Each condition of the simple fillet is compared to all the possibilities of each design of the standard, according to Equation (4), and presented respectively in Figure 9 and Figure 10 (d-f). For ease of understanding, the marker types are maintained for each simple fillet geometry.

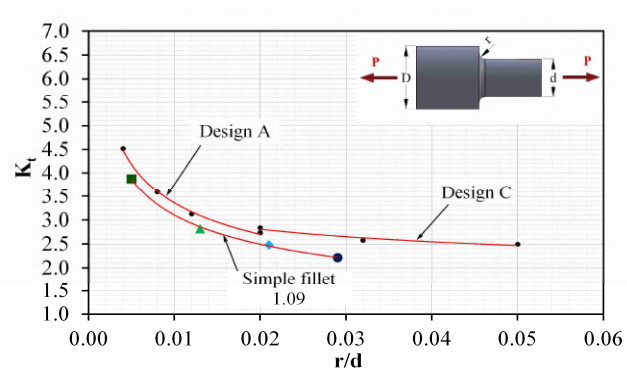


(a) Absolute values — for traction

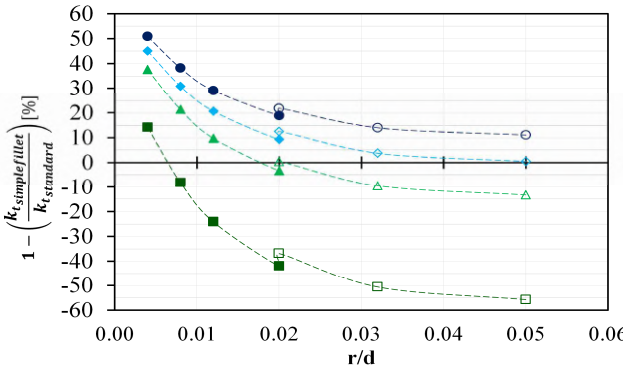


(d) Relative values based on the simple fillet — for traction

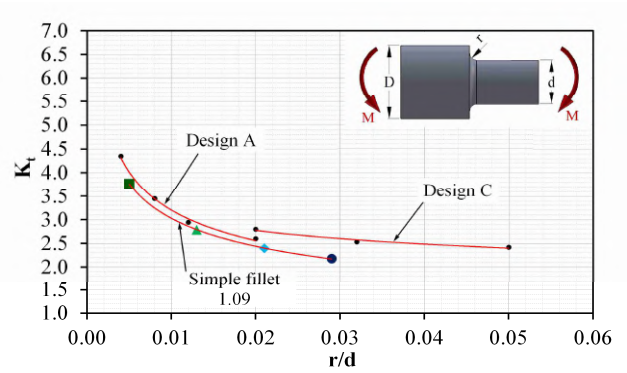


(b) Absolute values — for bending

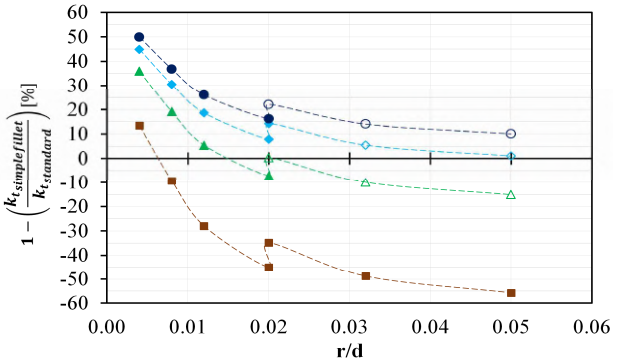


(e) Relative values based on the simple fillet — for bending

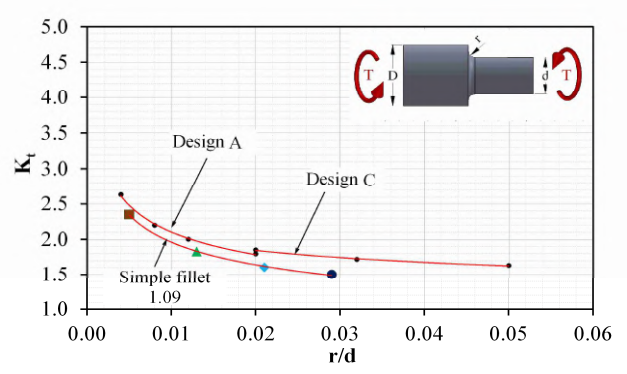


(c) Absolute values — for torsion

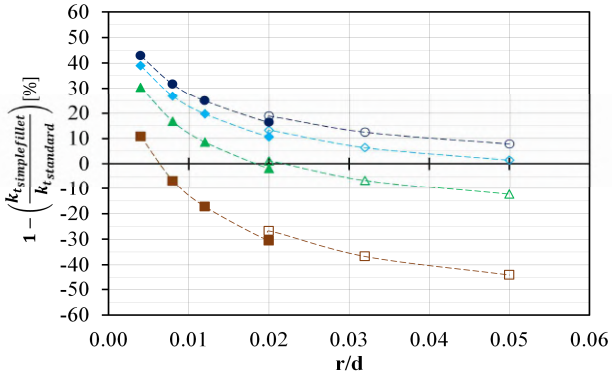


(f) Relative values based on the simple fillet — for torsion

Figure 9. Comparison of stress concentration factors between standard designs and simple fillet (D/d=1.09). Filled markers represent design A, while unfilled represent design C.

By this comparison it is clear that the standards benefit isn't always present, due to the majority of results being above the null axis, it is noted that for the *D/d=1.09* ratio, only 33.3 % of standards concentration factors were beneficial, this value being reduced to only 8 % when considering the *D/d=1.55* ratio. However, on points that do have beneficial properties, that is, are below the null axis, is seen a reduction of concentration factors reaching to almost 60 %. This result

is relevant, since the classic literature indicates that the application of shoulder designs would always have gained in relation to the stress concentration factor. However, the result shows that this is not valid in all cases, and it is possible to gain more critical cases where the constraint of assembly imposes relatively small radii for the simple fillet design.

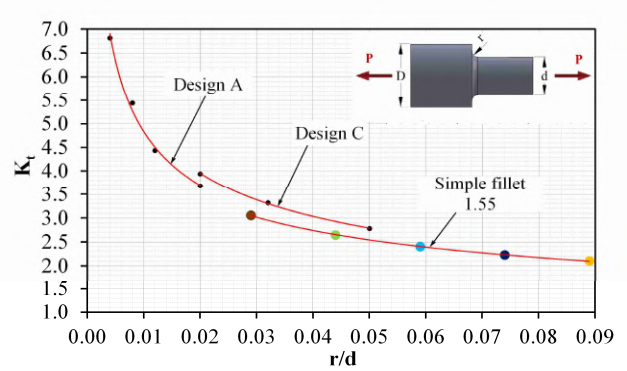


(a) Absolute values — for traction

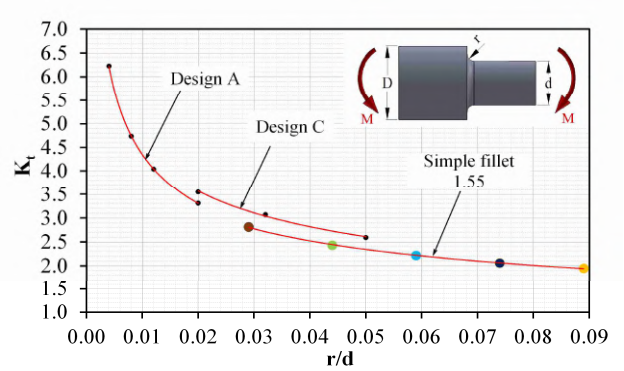


(b) Absolute values — for bending

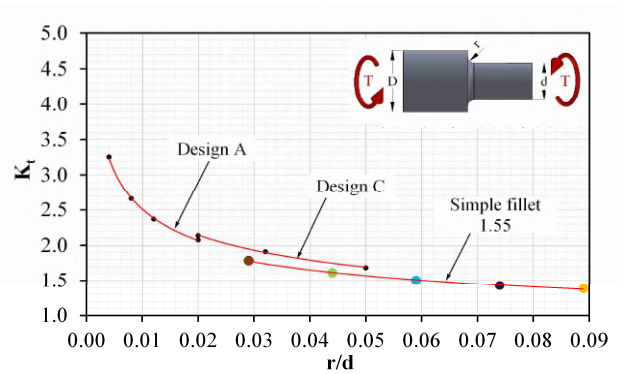


(c) Absolute values — for torsion

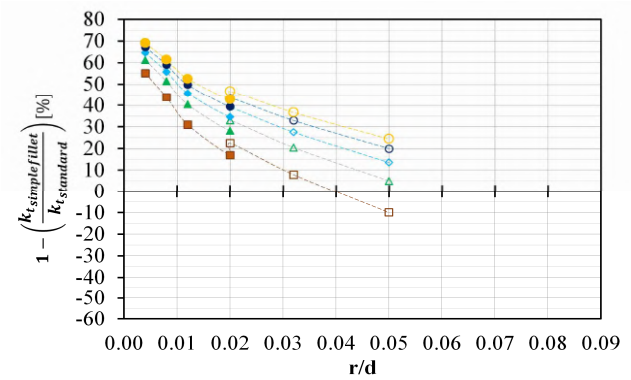


(d) Relative values based on the simple fillet — for traction

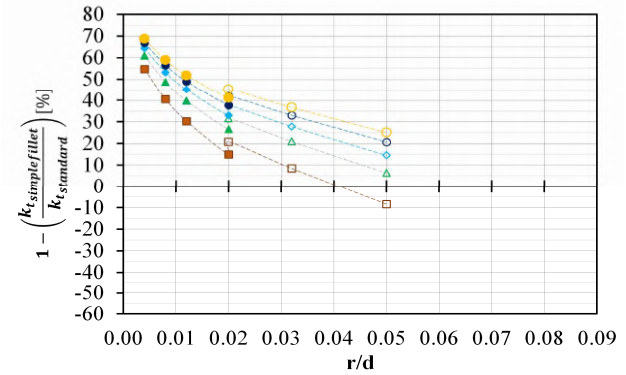


(e) Relative values based on the simple fillet — for bending

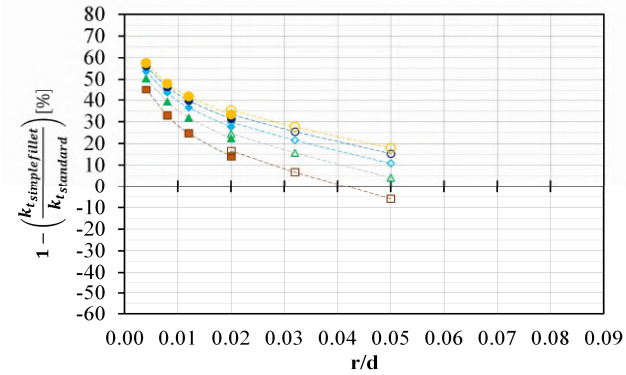


(f) Relative values based on the simple fillet — for torsion

Figure 10. Comparison of stress concentration factors between standard designs and simple fillet (D/d=1.55). Filled markers represent design A, while unfilled represent design C.

## 4. CONCLUSIONS

The current work had as objective the numerical evaluation of stress concentration factors in shafts, considering different designs of radial bearing shoulders and pure traction force, bending moment and torsion moment. In particular, two designs of shoulder bearings, proposed through a standard, with the simple fillet design were compared. The main contributions and conclusions were:

- The development and validation of a numerical methodology for evaluating stress concentration factors via Ansys®;
- The determination of a potential-type equation for measure of stress concentration factors considering the design A and C (DIN 509, 1998) for different geometric parameters that met the radial-bearing application ranges of

deep-groove ball bearings, cylindrical roller bearings, angular contact ball bearings, tapered roller bearing, self-aligning ball bearings, and self-aligning roller bearings;

- In relation to stress concentration factors for the simple fillet, designs A and C had an analogous behavior, with higher values presented for traction force and bending moment;
- A comparison, based on a percentage relation, between the stress concentration factors for the different designs in relation to the simple fillet;
- Comparatively, it was observed that, unlike pointed out in literature, the use of the simple fillet, in some cases, may present lower stress concentration factors than those generated by the designs A and C. In this case, relative values of the concentration factors indicated a dependence with the ratios of D/d.

## 5. REFERENCES

Abhyankar, A.A. and Deshmukh, G.P., 2017. "A review paper on stress concentration of shoulder fillet in shaft". *International Journal for Scientific Research & Development*, Vol. 4, No. 11, pp. 509–514.

Ajovalasit, A., Nigrelli, V., Pitarresi, G. and Mariotti, G.V., 2014. "On the history of torsional stress concentrations in shafts: From electrical analogies to numerical methods". *The Journal of Strain Analysis for Engineering Design*, Vol. 49, No. 6, pp. 452–466.

Allison, I.M., 1961. "The elastic stress concentration factors in shouldered shafts. Part I: Shafts subjected to torsion". *Aeronautical Quarterly*, Vol. 12, No. 2, pp. 189–199.

Deshpande, S.S., Desai, P. N., Pandey, K. P. and Pangarkar, N.P., 2016. "Detailed studies on stress concentration by classical and finite element analysis". *International Journal of Mechanical Engineering and Technology*, Vol. 7, No. 2, pp. 148–167.

DIN 509:1998-06. Technical drawings – Undercuts – Types and dimensions.

Hibbeler, R.C., 2015. Engineering Mechanics Statics, 13th Edition.

Norton, R.L., 2010. Machine Design An Integrated Approach - Robert L Norton, Prentice Hall ,4th edition.

Pilkey, W.D., Pilkey, D.F., 2008. Peterson's Stress Concentration Factors. Wiley Interscience, 3th edition.

SKF. General catalogue, 2003.

Yang, Z., Kim, C-B., Cho, C. and Beom, H.G., 2008. "The concentration of stress and strain in finite thickness elastic plate containing a circular hole". *International Journal of Solids and Structures*, Vol. 45, No. 3–4, pp. 713–731.

Young, W.C., Budynas, R.G., 2002. Roark's Formulas for Stress and Strain. McGraw-hill, 7th edition.

Zienkiewicz, O.C., Taylor, R.L., 2000. The Finite Element Method. Volume 1: The Basis. Butterworth Heinemann, 5th edition.

## 6. RESPONSIBILITY NOTICE

The authors are the only responsible for the printed material included in this paper.